Phase coherence in the current-carrying charge-density-wave state: ac-dc coupling experiments in $NbSe_3$

A. Zettl and G. Grüner
Department of Physics, University of California, Los Angeles, California 90024
(Received 13 May 1983)

Various experiments which involve the joint application of dc and ac driving fields, $V=V_{dc}+V_{ac}\cos(\omega t)$, are reported for the charge-density-wave (CDW) state of the linear-chain compound $NbSe_3$. Steps are observed in the dc I-V characteristics when ac driving fields are applied. The complex ac response $\sigma_{ac}(\omega)$ is also strongly influenced by the application of dc fields, with sharp changes occurring in $\sigma_{ac}(\omega)$ for well-defined driving frequencies and bias fields. These phenomena are the consequence of interference effects between the applied ac signal and the intrinsic current oscillations. In both cases, the ac "interference" frequency is proportional to the excess current I_{CDW} carried by the charge-density wave. We analyze our experiments in terms of a simple nonlinear equation proposed previously to account for the field- and frequency-dependent response and current oscillation phenomena. The equation is formally identical to the equation describing a resistively shunted Josephson junction (Stewart-McCumber model). Analysis in terms of this equation leads to a highly coherent sample response where the specimen can be described by a single degree of freedom. Our observations are also discussed in light of recent theories of CDW pinning and dynamics.

I. INTRODUCTION

It is by now well established that the strong nonlinearity of the dc conductivity $\sigma_{dc}(E)$ observed in the linear-chain trichalcogenides $NbSe_3$,[1] orthorhombic and monoclinic TaS_3,[2] and NbS_3 (Ref 3) is due to the current-carrying charge-density-wave (CDW) state. The CDW condensate, which is a consequence of electron-phonon interactions,[4] is characterized by a complex order parameter and can be represented in the familiar form

$$\Delta\rho(x)=A\cos(2k_Fx+\phi)\ , \tag{1}$$

where x refers to the chain direction, k_F is the Fermi wave vector, and A and ϕ are the amplitude and phase of the CDW condensate. With a condensate characterized by an amplitude and by a phase, both amplitude and phase excitations are possible. The minimum energy for amplitude excitations is given by[5] $\Omega^+=g^{1/2}\omega_{2k_F}$ where g is the dimensionless electron-phonon coupling constant and ω_{2k_F} is the phonon frequency at $2k_F$. The period of the CDW, $\lambda=\pi/k_F$, is determined by the band filling, and thus the CDW may be commensurate or incommensurate with the underlying lattice.

For an incommensurate CDW, such as develops in $NbSe_3$ in both charge-density-wave states, the phase can, in the absence of various pinning mechanisms, be arbitrary with respect to the underlying lattice. In this case, the energy of the system is phase independent. With an arbitrary phase, arbitrarily small applied electric fields can lead to a current carried by the CDW condensate. Various mechanisms, however, lead to pinning of the CDW and thus to a nonconducting state for low dc driving fields.[6] In $NbSe_3$ and in TaS_3 (orthorhombic form) pinning is provided by residual impurities in the specimens.[7,8] Although the detailed mechanism of impurity pinning is not clear, various estimates lead to pinning energies orders of magnitude smaller than the energies which correspond to the single-particle gap Δ in the electronic dispersion relation or to the energy Ω^+ associated with the energy of the amplitude mode.[9]

The pinned mode displays strongly frequency-dependent response and a very large dielectric constant.[10,11] Moreover, the CDW can be depinned by small applied dc electric fields exceeding a threshold field E_T (Ref. 1) leading to a current-carrying CDW state as originally suggested by Fröhlich.[12] In the current-carrying state an oscillating component of the current is observed for applied dc fields exceeding E_T. These oscillations have been investigated both in the frequency domain[13] and in the time domain.[14,15] The sharp peaks observed in the former case are referred to as "narrow-band-noise" peaks. The dominant frequency f_1 of the current oscillations is proportional to the current carried by the CDW and recent experiments[16,17] are in agreement with the expression

$$I_{CDW}=\frac{n(T)}{n(T=0)}cf_1\ , \tag{2}$$

where $n(T)$ is the number of carriers per unit length in the CDW condensate and c is a constant.

Various models have been proposed to account for these experimental findings; two models attempt to describe the observations in detail. A phenomenological model[18,19] treats the CDW as a classical object of mass m and charge e moving in a periodic potential where the period is given by the CDW period λ. The equation of motion is

$$\frac{d^2x}{dt^2}+\frac{1}{\tau}\frac{dx}{dt}+\frac{\omega_0^2}{Q}\sin(Qx)=\frac{eE}{m}\ , \tag{3}$$

where $\tau^{-1}=\gamma/m$, with γ the damping constant, $\omega_0^2=k/m$, with k the restoring force constant, and $Q=2\pi/\lambda$. E is the applied electric field. Although the

classical model does not account for the pinning mechanism (a rigid CDW is not expected to be pinned by randomly distributed impurities in the thermodynamic limit[20]), it describes the overall qualitative features of the frequency-dependent response of the pinned mode, and also the observed nonlinear conductivity when E exceeds the threshold field E_T. It also accounts for the current oscillation phenomena, and predicts the linear relation between $I_{\rm CDW}$ and f_1 as given by Eq. (2). In addition the model accounts well for the results of various experiments involving the joint application of ac and dc driving fields, such as the low-field dc conductivity in the presence of an applied ac field.[21] The model leads, however, to spurious divergences if $E \rightarrow E_T$ from below. For example, the differential conductivity dI/dV diverges if $E \rightarrow E_T$ from below threshold, although these divergences have not been obtained by experiment. The phenomenological classical model is closely related to an electrical analog, the relaxation oscillator.[22] This electrical analog also reproduces the overall features of the experimental findings, with again exception to the divergences predicted near E_T.

An alternative model proposed by Bardeen[23] assumes that the pinning can be represented by a gap in the (pinned) CDW excitation spectrum. Excitation of the CDW across the gap by dc and/or ac fields leads to field- and frequency-dependent transport phenomena. The former is similar to (single-particle) Zener tunneling, and a theory developed by Tucker for superconducting-insulating-superconducting (SIS) junctions[24] is used to evaluate the frequency-dependent response. Both $\sigma_{\rm ac}(\omega)$ and $\sigma_{\rm dc}(E)$ can be described in detail by the postulated formulas of Bardeen's tunneling model.[23] Assuming a coherent sliding CDW motion over the valleys and hills of the pinning potential, the current oscillation phenomena can also be accounted for, and energy-conservation arguments lead to a pinning potential in good agreement with that obtained from the frequency-dependent response.[15] Bardeen's model[23] also accounts[25] for ac-dc coupling and microwave harmonic mixing experiments.[26] Predicted quantum phenomena such as photon-assisted tunneling[27] have, however, not been observed to date, and reasons for the failure of the tunneling model in these cases have been summarized by Bardeen.[23]

We believe that in the classical limit both formalisms should give an overall qualitative account of experiments for a broad parameter range. Both the classical and tunneling models should, for example, describe phenomena associated with the intrinsic oscillations produced by the moving CDW.

In this paper the basis of analysis for our experimental data will be the classical model, Eq. (3), which can be solved under a number of parameter conditions applied experimentally, allowing a direct comparison with experiments. We stress, however, that the semiconductor or tunneling model[23] is also expected to give a good account of our experimental findings.

The substitution $\theta = Qx$ allows Eq. (3) to be reduced to the dimensionless form

$$\frac{d^2\theta}{dt^2} + \Gamma \frac{d\theta}{dt} + \sin\theta = \frac{E}{E_T} , \tag{4}$$

where $\Gamma = (\omega_0 \tau)^{-1}$, $E_T = (\lambda/2\pi)\, m\omega_0^2/e$, and time t is measured in units of ω_0^{-1}. Equation (4) is formally identical to the equation which describes the behavior of resistively shunted Josephson junctions,[28]

$$\frac{d^2\phi}{dt^2} + G\frac{d\phi}{dt} + \sin\phi = \frac{I}{I_J} , \tag{5}$$

where ϕ is the phase difference across the junction, I is the current through the junction, $G = (RC\omega_J)^{-1}$, where R and C are the resistance and capacitance of the junction, and $\omega_J = 2eI_J/C\hbar$. I_J is the dc critical Josephson current, and time is measured in units of ω_J^{-1}. This formal analogy, also recognized by others,[29] suggests a close correspondence between phenomena observed in Josephson junctions and in materials displaying CDW transport. For example, the current oscillations described by Eq. (2) correspond to the ac Josephson effect.

In this paper we report observations of the CDW response in $NbSe_3$ in the presence of joint dc and ac driving fields,

$$V = V_{\rm dc} + V_{\rm ac}\cos(\omega t) . \tag{6}$$

Various types of experiments have been performed and analyzed in detail, and most correspond to experiments well known in the Josephson literature.[29] According to the nature of the excitation and mode of detection, we may classify these experiments as follows.

(i) The effects of ac field on the dc I-V characteristics: $V_{\rm ac}$ and ω are held constant, $V_{\rm dc}$ is varied, and $I_{\rm dc}$ is detected.

(ii) The effect of dc field on the ac response: $V_{\rm dc}$ and $V_{\rm ac}$ are held constant, ω is varied, and $I_{\rm ac}$ of frequency ω is detected.

(iii) The effect of swept dc field on the ac response: $V_{\rm ac}$ and ω are held constant, $V_{\rm dc}$ is varied, and $I_{\rm ac}$ is detected.

In experiments (ii) and (iii), from the measured $I_{\rm ac}$ and applied $V_{\rm ac}$ the real and imaginary parts of the conductivity are evaluated using

$$\sigma_{\rm ac}(\omega) = {\rm Re}\sigma_{\rm ac}(\omega) + i\,{\rm Im}\sigma_{\rm ac}(\omega) = \frac{I_{\rm ac}(\omega)}{V_{\rm ac}} . \tag{7}$$

It should be mentioned that due to the inherent nonlinearity of the problem, an applied sinusoidal voltage does not lead to a sinusoidal response for finite $V_{\rm ac}$ values. The linear approximation is, however, appropriate for small applied ac fields in the $V_{\rm ac} \rightarrow 0$ limit, and our experiments were performed in this limit. The dc conductivity is defined as $\sigma_{\rm dc} = I_{\rm dc}/V_{\rm dc}$.

The broad variety of experimental observations can (perhaps somewhat arbitrarily) be classified into two groups: first, the overall modification of the dc or ac response by the joint application of ac or dc driving fields, and second, interference phenomena between the intrinsic current oscillations and the externally applied ac field. Although we shall briefly comment on the overall dependence of the ac and dc responses as functions of the excitation amplitudes and frequency, in this paper we shall focus on the interference phenomena in the current-carrying CDW state. A comparison of our experimental

findings with expressions worked out originally for Josephson junctions[29] suggests a highly coherent response and demonstrates the development of long-range phase coherence in the sliding CDW mode, in agreement with conclusions drawn from our previous analysis of current-oscillation phenomena[15] in $NbSe_3$.

Experiments concerning interference effects have been performed previously by Monceau *et al.*[16] who have reported sharp steps in the differential resistance dV/dI due to the application of ac fields. Some of our experiments are the extension of these studies to larger applied ac fields and frequencies. Also, the effects observed by us are approximately 2 orders of magnitude larger than those reported by Monceau *et al.*[16] We believe that this is due to a higher sample quality and more well-defined sample geometries for our samples. Some of our experiments have been reported earlier.[30,31]

II. EXPERIMENTAL DETAILS AND RESULTS

The experiments were performed both on $NbSe_3$ samples provided by Fleming (Bell Laboratories) and $NbSe_3$ samples prepared by ourselves. Typical crystal dimensions were 1 mm$\times$10 μm$\times$1 μm with the long dimension corresponding to the highly conducting chain axis. Our conductivity measurements are with respect to this axis. All experiments were carried out in the lower CDW state, i.e., below the second phase transition which occurs at $T_2=59$ K. In all experiments the applied voltages were smaller than those needed to depin both CDW's and consequently our experiments are described in terms of the dynamics of one CDW. Although we performed experiments at various temperatures below T_2, most of the experimental data reported here were taken at temperature $T=42$ K, which is near the temperature where the Ohmic resistance has a local maximum and the threshold voltage V_T attains its minimum value.[1]

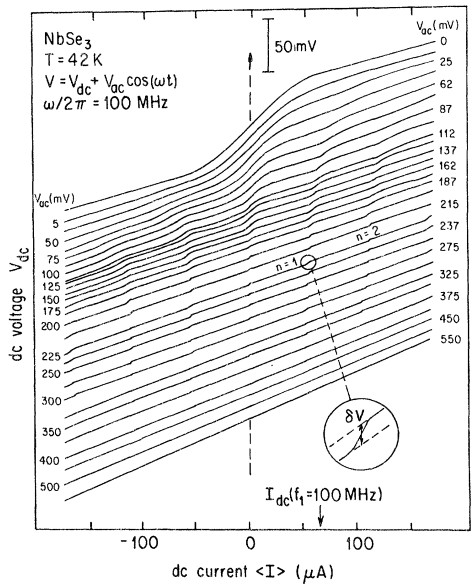

FIG. 1. dc I-V traces for $NbSe_3$ at 42 K in the presence of an applied rf field at frequency $\omega/2\pi=100$ MHz and of amplitude V_{ac}. Step height δV is defined in the figure. No Shapiro steps are seen for $V_{ac}=0$, while the maximum step height is at approximately $V_{ac}=100$ mV. Arrow indicates the dc current which yields a noise frequency $f_1=100$ MHz. n is the step index (see text).

Both the real and imaginary parts of the ac conductivity, $\mathrm{Re}\sigma_{ac}(\omega)$ and $\mathrm{Im}\sigma_{ac}(\omega)$, were measured with an HP 8754A network analyzer. The technique involved terminating a 50-Ω coaxial cable with an $NbSe_3$ crystal, and then measuring the complex reflection coefficient of the cable termination. Both the ac driving frequency ω and the dc bias field E_{dc} could be swept continuously during the measurement process; $\omega/2\pi$ could be varied between 4 and 500 MHz and E_{dc} between zero and approximately 20 times E_T. For larger dc bias fields, self-heating of the sample became apparent. For the experimental results reported here, the amplitude V_{ac} of the ac driving field was held at a value substantially smaller than V_T, the threshold voltage for nonlinear dc conductivity, measured in the absence of an ac driving field. Our measurement setup also allowed us, during the same experimental run, to measure the response of the sample to pulsed dc electric fields. With the use of a pulse method,[15] we were able to observe directly on an oscilloscope the amplitude and frequency of the coherent current oscillations as functions of the applied electric field. Measurements of $\sigma_{dc}(V_{dc})$ by pulse method also verified that heating effects were unimportant up to $20V_T$ for continuously applied dc fields.

We shall first discuss experiments which fall into the first category as outlined earlier, i.e., a modification of the dc I-V characteristics of the sample by an applied ac field. Figure 1 shows several dc I-V traces for $NbSe_3$ at $T=42$ K. The excitation applied to the sample was of the form $V=V_{dc}+V_{ac}\cos(\omega t)$ with $\omega/2\pi=100$ MHz. For $V_{ac}=0$, a smooth, nonlinear I-V curve is observed with a well-defined threshold voltage V_T where the conductivity starts to be nonlinear. At higher values of V_{ac}, well-defined steps, which we shall index with an integer n, appear in the nonlinear region. The step height δV, as defined in the figure, in general first increases with increasing V_{ac} and then decreases. The position of $n=1$ step (identified in the figure) corresponds to a dc current I_{dc} which, in the absence of ac fields, yields an intrinsic oscillation of frequency $f_1=100$ MHz$=\omega/2\pi$. This has been established by measuring the oscillation frequency directly with the method described in Ref. 15. We also note the presence of harmonic steps corresponding to $n=2$ (where $f_1=200$ MHz) and smaller subharmonic steps corresponding to $n=\frac{1}{2}$ (where $f_1=50$ MHz). The steps are thus clearly an interference effect between the intrinsic current oscillation and the externally applied rf excitation. In Fig. 2 we show the results of the same experiments on a second sample with ac applied frequency $\omega/2\pi=210$ MHz. In Fig. 2 the $n=1$ steps are clearly visible.

The definition of the step height, as indicated in Fig. 1, is straightforward and we shall strictly adhere to it in the analysis section of this report. However, for steps corresponding to $n>2$ the steps in the I-V curves become difficult to observe directly. A more sensitive test for higher harmonic steps is to detect the differential resistance dV/dI of the sample (using a very-low-frequency ac

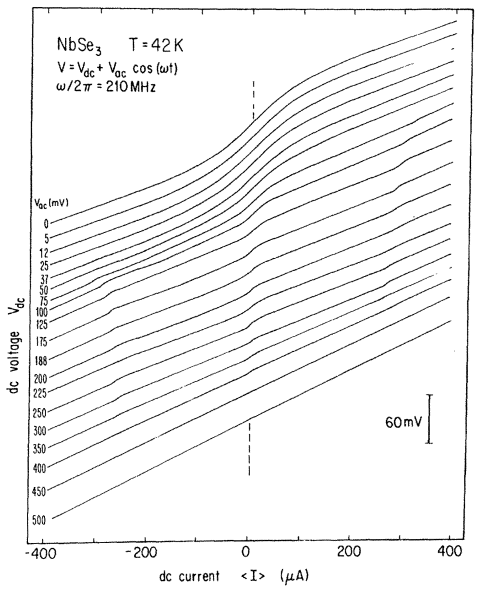

FIG. 2. dc I-V traces for $NbSe_3$ at 42 K in the presence of an applied rf field at frequency $\omega/2\pi=210$ MHz and of amplitude V_{ac}. Steps corresponding to $n=1$ are clearly seen for moderate values of V_{ac}.

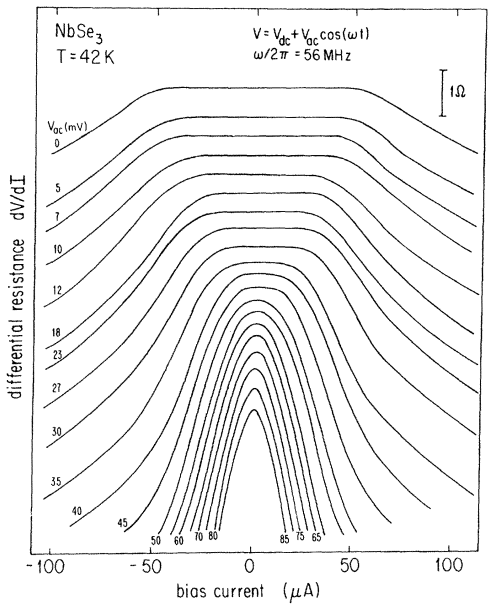

FIG. 4. Differential resistance dV/dI of $NbSe_3$ at $T=42$ K for various amplitudes V_{ac} of an applied rf signal at frequency $\omega/2\pi=56$ MHz. dc threshold voltage V_T goes smoothly to zero with increasing V_{ac}.

modulation of small amplitude) in the presence of a dc bias field and rf radiation. This is shown in Fig. 3 for again a different $NbSe_3$ sample at $T=42$ K. Figure 3 shows data for several different values of V_{ac} with $\omega/2\pi=5$ MHz. In this plot, steps corresponding to values as high as $n=15$ are apparent, along with subharmonic steps. Similar to the step-height observations of Figs. 1 and 2, the $n=1$ peak (identified with an arrow) in general first increases and then decreases with increasing V_{ac}. It should be noted, however, that the heights of the peaks in dV/dI do *not* correspond directly to the height δV as defined in Fig. 1. Rather, the peak heights in Fig. 3 reflect the "sharpness" of the steps in the direct I-V characteristics.

Experiments such as those shown in Figs. 1–3 were performed at various applied ac frequencies between $\omega/2\pi=1$ and 210 MHz. Owing to instrumental limitations, we did not extend our experiments to higher frequencies, although (as discussed later) such higher-frequency measurements are desirable.

In addition to inducing steps on the dc I-V characteristics of the sample, the application of an ac field also changes V_T, the threshold voltage for the onset of nonlinear conduction. Although this effect is observable in

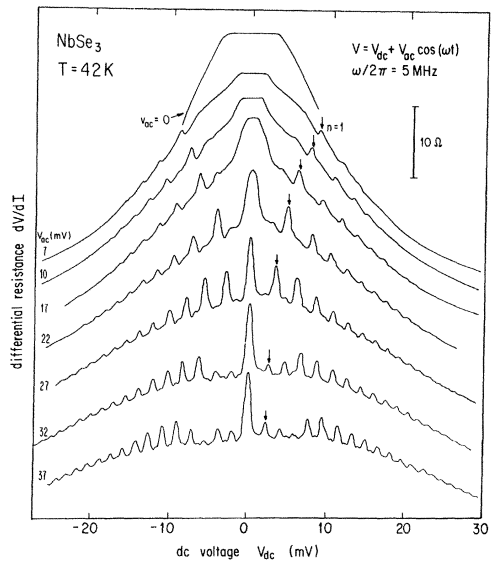

FIG. 3. Differential resistance dV/dI of $NbSe_3$ at $T=42$ K in the presence of an applied rf field at frequency $\omega/2\pi=5$ MHz. $n=1$ Shapiro step is identified with an arrow (see text).

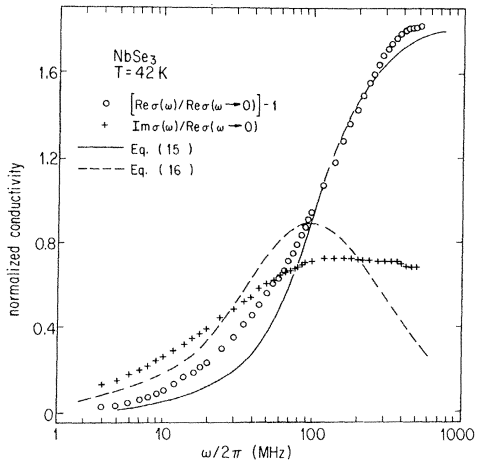

FIG. 5. Real and imaginary parts of the conductivity $Re\sigma_{ac}(\omega)$ and $Im\sigma_{ac}(\omega)$ at 42 K in the absence of applied dc field. ac test signal amplitude V_{ac} was much smaller than the dc threshold voltage V_T.

Figs. 1–3, it is shown more dramatically in Fig. 4, which shows the differential resistance dV/dI of a $NbSe_3$ sample for various values of V_{ac} and for $\omega/2\pi=56$ MHz. These data were obtained by sweeping the dc bias current I_{dc} and measuring dV/dI (again using a low-field and low-frequency ac modulation) in the presence of rf radiation. Figure 4 shows clearly that in the presence of an ac field, V_T smoothly goes to zero with increasing V_{ac}.

We now turn to experiments of the second type as categorized above, namely the effect of a dc bias field on the ac conductivity $\sigma_{ac}(\omega)$. The experiments which involve the measurement of the ac response in the presence of dc fields were performed after experiments on the field- and frequency-dependent conductivity were completed. The threshold for the onset of dc nonlinear conduction V_T was established by measuring the dc I-V characteristics. In Fig. 5 we show for zero dc bias the real and imaginary parts of the ac conductivity, $\mathrm{Re}\sigma_{ac}(\omega)$ and $\mathrm{Im}\sigma_{ac}(\omega)$. For the data displayed in Fig. 5 the applied ac amplitude V_{ac} was more than an order of magnitude smaller than V_T; therefore, $\mathrm{Re}\sigma_{ac}(\omega)$ and $\mathrm{Im}\sigma_{ac}(\omega)$ as shown correspond to the ac response in the small amplitude "linear" regime of the pinned CDW mode where both $\mathrm{Re}\sigma_{ac}(\omega)$ and $\mathrm{Im}\sigma_{ac}(\omega)$ are independent of V_{ac}.

Figures 6 and 7 show as a function of applied dc bias the real and imaginary parts of the complex conductivity, $\mathrm{Re}\sigma_{ac}(\omega)$ and $\mathrm{Im}\sigma_{ac}(\omega)$, measured at $\omega/2\pi=3.2$ MHz. It is evident that neither the real nor the imaginary part of the frequency-dependent response is strongly affected by an applied dc voltage as long as $V_{dc}<V_T$. However, for $V_{dc}>V_T$, $\mathrm{Re}\sigma_{ac}$ ($\omega/2\pi=-=3.2$ MHz) strongly increases and the ac dielectric constant ϵ ($\omega/2\pi=3.2$ MHz) strongly decreases for increasing V_{dc}. The dielectric constant is related to the ac conductivity by

$$\epsilon(\omega)=\frac{4\pi\,\mathrm{Im}\sigma_{ac}(\omega)}{\omega}\ . \tag{8}$$

The dielectric constant approaches zero above $V_{dc}\sim 3V_T$, showing that there is no appreciable out-of-phase component at high applied dc voltages. $\mathrm{Re}\sigma_{ac}(\omega)$, on the other hand, approaches the high-frequency limit obtained from the frequency dependence of $\mathrm{Re}\sigma_{ac}(\omega)$ as shown in Fig. 5.

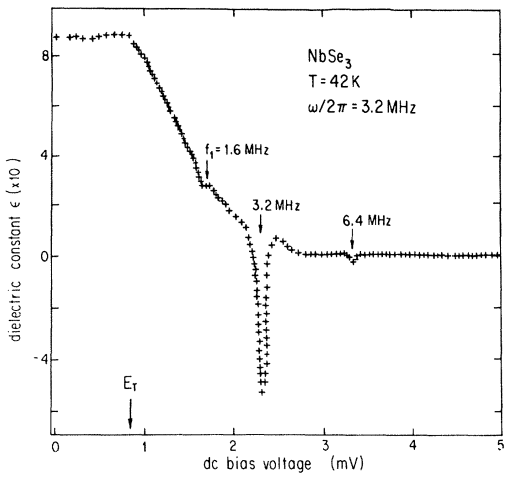

FIG. 7. ac dielectric constant $\epsilon(\omega)$ measured at $\omega/2\pi=3.2$ MHz as a function of applied dc bias voltage. Threshold field E_T for the onset of nonlinear conduction is indicated by an arrow.

In addition to the overall behaviors described above, Figs. 6 and 7 also show that for $NbSe_3$ both $\mathrm{Re}\sigma_{ac}(\omega)$ and $\epsilon(\omega)$ have sharp anomalies for well-defined values of V_{dc} in the nonlinear conductivity region. Specifically, $\mathrm{Re}\sigma_{ac}$ shows "steps" to higher conductivity values at $V_{dc}=1.6$, 2.3, and 3.3 mV. At these same values of V_{dc}, ϵ shows well-defined inductive dips. The dip at $V_{dc}=2.3$ mV is especially dramatic, and at this field $\mathrm{Re}\sigma_{ac}$ also shows the largest conductivity step. It is important to clearly distinguish the steps and dips shown in Figs. 6 and 7 from the steps in the I-V characteristics discussed before. The steps shown in Figs. 1–3 are steps in the dc I-V characteristics due to applied large amplitude ac fields (i.e.,

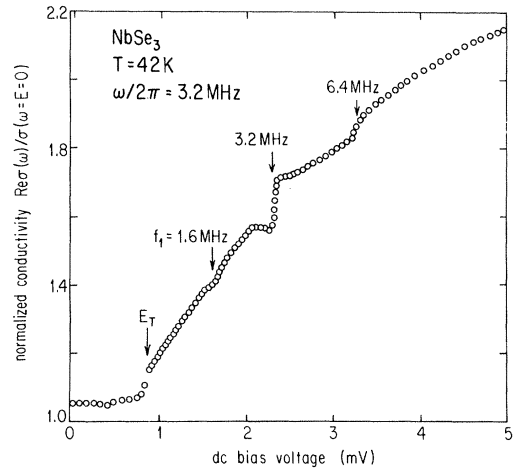

FIG. 6. Real part of the ac conductivity $\mathrm{Re}\sigma_{ac}(\omega)$ measured at $\omega/2\pi=3.2$ MHz as a function of applied dc bias voltage. Threshold field E_T for the onset of nonlinear dc conduction is indicated by an arrow.

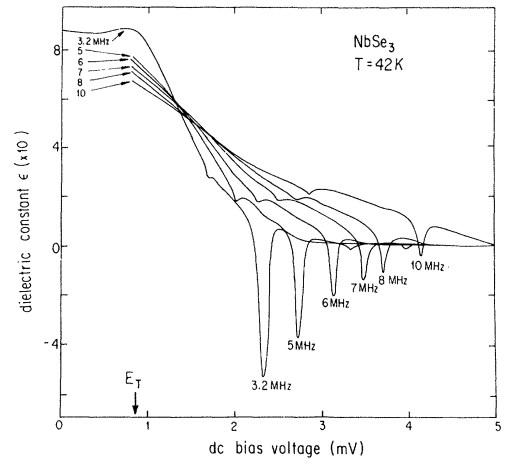

FIG. 8. ac dielectric constant $\epsilon(\omega)$ measured at various ac frequencies as a function of applied dc bias voltage. Negative dielectric constant indicates inductive response. Threshold field E_T for the onset of nonlinear dc conduction is indicated by an arrow.

$V_{ac} \gg V_T$). In Figs. 6 and 7 we are dealing with anomalies in the low-field ac response due to an applied dc field.

The position of the steps in $\mathrm{Re}\sigma_{ac}$ and corresponding dips in ϵ, as seen in Figs. 6 and 7, are sensitive functions of ω, the ac driving and detection frequency. As ω is increased the steps and dips move progressively to higher V_{dc} values. This is shown in Fig. 8 where ϵ has been plotted for several values of ω. For a given ac frequency ω, the strong step in $\mathrm{Re}\sigma_{ac}$ and large dip in ϵ appears at a value of V_{dc} which by itself produces a coherent current oscillation of fundamental frequency $f_1 = \omega/2\pi$. This is illustrated in Fig. 9 where the position of the strong inductive dip has been plotted as a function of ω. Instead of labeling the position of the dip by V_{dc}, the excess CDW current I_{CDW} has been used. I_{CDW} is a well-defined function of V_{dc} obtained from the dc I-V characteristics of the sample. From Fig. 9, we see that a linear relation exists between ω and I_{CDW} up to $\omega/2\pi = 100$ MHz. Beyond 100 MHz it was not possible to resolve the inductive dip in the $\epsilon(\omega, V_{dc})$ data. Figure 9 also shows, for the same sample, the fundamental frequency f_1 of the coherent current oscillations. f_1 was determined from direct observation of the oscillating component of I_{CDW} on an oscilloscope and is seen to be proportional to I_{CDW}. What is important here is that in Fig. 9 the data points for $\omega/2\pi$ and f_1 fall on the same line, clearly indicating that the steps in $\mathrm{Re}\sigma_{ac}(\omega, V_{dc})$ and inductive dips in $\epsilon(\omega, V_{dc})$ are the result of a direct coupling between the ac driving field at frequency $\omega/2\pi$ and the current oscillations at fundamental frequency f_1. The smaller steps and dips, as shown at $V_{dc} = 1.6$ and 3.3 mV in Fig. 7, indicate subharmonic and harmonic interference effects. These anomalies occur at dc bias fields where f_1 equals $\frac{1}{2} \times (\omega/2\pi)$ and $2 \times (\omega/2\pi)$, respectively. In short, for a detection frequency $\omega/2\pi$, interference effects are observed whenever the fundamental noise frequency $f_1 = \omega/2\pi$ or is a harmonic or subharmonic of $\omega/2\pi$.

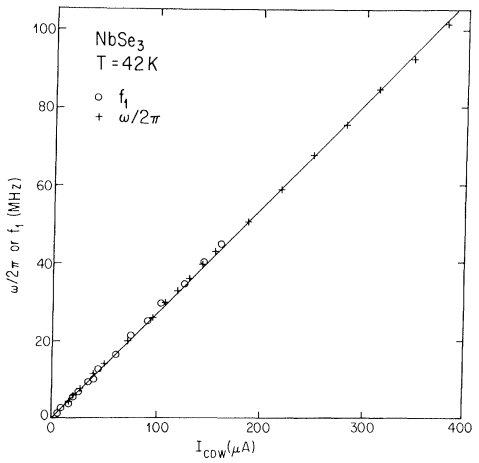

FIG. 9. ac interference frequency $\omega/2\pi$ as a function of excess CDW current I_{CDW}. Interference frequency is defined as the frequency which leads to the inductive dip at V_{dc} in $\epsilon(\omega, V_{dc})$. V_{dc} is related to I_{CDW} through the dc I-V characteristics of the sample. Also plotted is f_1, the fundamental narrow-band noise frequency.

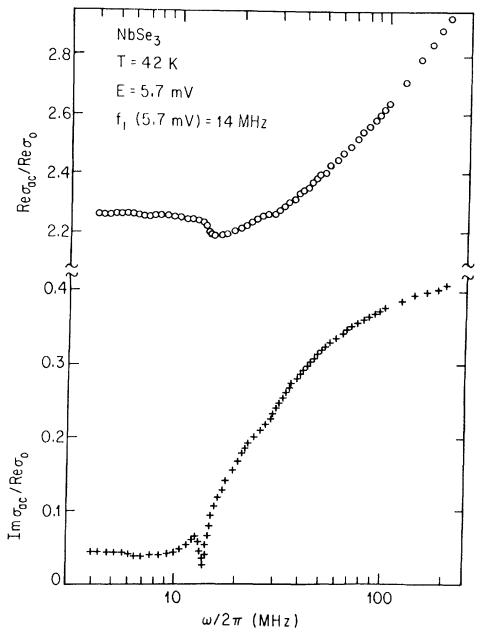

FIG. 10. Real and imaginary parts of the ac conductivity $\sigma_{ac}(\omega)$ of $NbSe_3$ as functions of frequency in the presence of applied dc bias. Fundamental noise frequency corresponding to this bias field is indicated in the figure.

The interference effects shown in Figs. 6 and 7 have been observed by detecting the ac response for a fixed frequency ω and a varying dc bias V_{dc}. Clearly, the same effects should be observable if V_{dc} is fixed at some value above V_T, and the ac response is measured as a function of ω. This is shown in Fig. 10, again for $NbSe_3$ at $T = 42$ K. The sample has been biased at $V_{dc} = 5.7$ mV, which yields an intrinsic oscillation frequency $f_1 = 14$ MHz. Interference effects in $\mathrm{Re}\sigma_{ac}(\omega)$ and $\mathrm{Im}\sigma_{ac}(\omega)$ are clearly

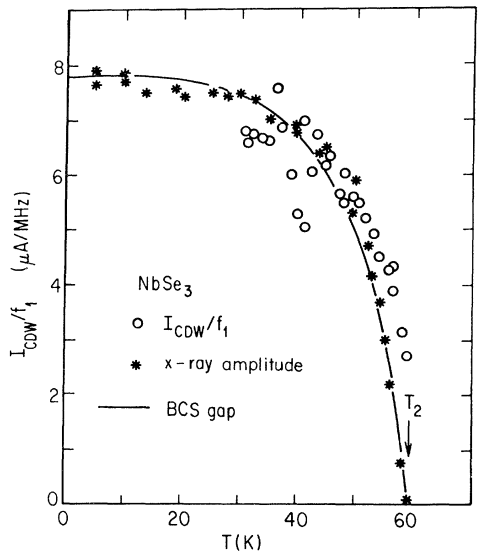

FIG. 11. I_{CDW}/f_1 for $NbSe_3$ at various temperatures below $T_2 = 59$ K. This ratio reflects the CDW order parameter $\Delta(T)$. Also plotted are the BCS gap expression for Δ and the x-ray superlattice amplitude as determined by Fleming (Ref. 42).

seen at $\omega/2\pi=7$ MHz$=\frac{1}{2}f_1$, 14 MHz$=f_1$, and 28 MHz$=2f_1$, as indicated by the arrows in Fig. 10. An experiment of this type falls into the third category of ac-dc coupling experiments as defined earlier.

The interference effects reported above have been observed at various temperatures in $NbSe_3$ and also in TaS_3.[32] In dealing with the temperature dependence of the phenomena, we shall, however, consider here only the temperature dependence of the f_1-vs-I_{CDW} relation. This ratio is of fundamental importance to the theory of CDW transport.

As shown in Fig. 9, the fundamental oscillation frequency f_1 in the nonlinear conductivity region is directly proportional to I_{CDW}, the excess current carried by the CDW. Data similar to that shown in Fig. 9 have been obtained at various temperatures in $NbSe_3$, and Fig. 11 shows the ratio I_{CDW}/f_1 as a function of temperature obtained from this data. Figure 11 clearly indicates that the ratio I_{CDW}/f_1 smoothly approaches zero as T approaches $T_2=59$ K from below. As we have mentioned earlier, this ratio can be interpreted as reflecting the concentration of carriers condensed in the CDW mode, $n(T)$.

III. ANALYSIS

In this section we analyze our experimental findings in terms of the simple nonlinear expression, Eq. (4). As remarked before, this equation is formally equivalent to the equation which describes the behavior of resistively shunted Josephson junctions.[33] Our experimental findings have close analogies to experimental results widely known and discussed in the Josephson literature.[30] Consequently, we will rely heavily on the theoretical predictions of models which have been worked out to interpret experiments performed on Josephson junctions.

First, the effect of the applied ac field on the dc nonlinear behavior will be discussed. Analogous effects are observed in Josephson junctions, and in particular the steps observed in the Josephson case are called Shapiro steps.[34] Effects analogous to the modification of the ac response (Figs. 6–8) have also been observed in Josephson junctions by measuring the changes in the properties of microwave resonant cavities.[30,35] However, due to limitations related to the calibration of microwave detecting systems, only qualitative analyses have been previously performed. We also interpret our experimental findings of the modification of the ac response by a dc bias in a phenomenological semiqualitative way. Finally, the relation between the fundamental noise frequency f_1 and the excess current I_{CDW} is discussed with regard to various theories of CDW transport.

A. ac induced steps in the dc I-V curves

In the Stewart-McCumber model of Josephson tunneling,[28] as described by Eq. (5), a driving current of the form $I=I_{dc}+I_{ac}\cos(\omega t)$ will produce steps in the dc I-V characteristics of the junction whenever the junction voltage $\langle V\rangle$ equals $n\hbar\omega/2e$, where n is an integer and $\omega/2\pi$ is the frequency of the ac component of the driving current. These steps are a direct consequence of the ac Josephson effect. Subharmonic steps corresponding to nonintegral values of n are also predicted under certain conditions.[36] The step height δI for the nth step can be obtained by explicitly solving Eq. (5). In the high-frequency limit ($\omega\gg 2eI_JR/\hbar$), computer simulations and analytic approximations show[30,37] that the height of the nth step is given approximately by

$$\delta I(\omega)\approx 2I_J(\omega=0)\,|J_n(I_1(\omega)/\omega GI_J(\omega=0))|\ . \tag{9}$$

The critical current I_J thus displays a dependence on the applied ac current given by

$$I_J(\omega)/I_J(\omega=0)=|J_0(I_1(\omega)/\omega GI_J(\omega=0))|\ . \tag{10}$$

In Eqs. (9) and (10), J_n is the Bessel function of order n. The corresponding equations for a CDW system are, by direct analogy to Eqs. (9) and (10),

$$\delta V=2V_T(\omega=0)\,|J_n(V_{eff})| \tag{11}$$

and

$$V_T/V_T(\omega=0)=|J_0(V_{eff})|\ , \tag{12}$$

with

$$V_{eff}=\frac{V_{ac}\omega_0^2\tau}{V_T(\omega=0)}\ . \tag{13}$$

The above equations have been derived in the high-frequency limit for a strongly damped system where the capacitive term (Josephson-junction case) or inertial term (CDW case) can be neglected. We note that Eq. (11) predicts that the maximum step height δV_{max} depends only on the maximum value of J_n and is thus independent of frequency ω. In the low-frequency limit, still neglecting the junction capacitance or CDW inertia, computer calculations[30,37] have yielded solutions for the step heights in the I-V characteristics which closely resemble Bessel functions. In this low-frequency limit the maximum step height δV_{max} is a strong function of frequency ω.

Equations (11)–(13) are appropriate to a coherent response with the whole specimen responding to the ac and dc driving fields as one coherent unit in the current-carrying state. If we assume that (due to either a distribution of the parameters which represent the CDW response or inhomogeneities such as phase boundaries, etc.) only a fraction α of the sample responds collectively to the external field, then Eq. (11) becomes

$$\delta V=2\alpha V_T(\omega=0)\,|J_n(V_{eff})|\ , \tag{14}$$

while Eq. (12) remains unchanged.

In order to properly evaluate the data shown in Figs. 1–3, in terms of Eq. (4), we must determine if we are in the high- or low-frequency regime. From Fig. 5, we see that the zero-bias ac conductivity $\sigma_{ac}(\omega)$ indicates a cross-over frequency $\omega_0^2\tau/2\pi\approx 100$ MHz. Thus, to evaluate data above approximately 200 MHz, we may use Eqs. (11)–(14), while for lower-frequency data the low-frequency computer solutions[30,37] of the resistively-shunted-junction (RSJ) model[28] are most appropriate.

In Fig. 12 we have plotted the step height of the $n=1$ steps of Fig. 2 as a function of the ac amplitude V_{ac}. This data is for $\omega/2\pi=210$ MHz, and thus we compare this data to Eq. (14). The solid line in Fig. 12 is Eq. (14), with

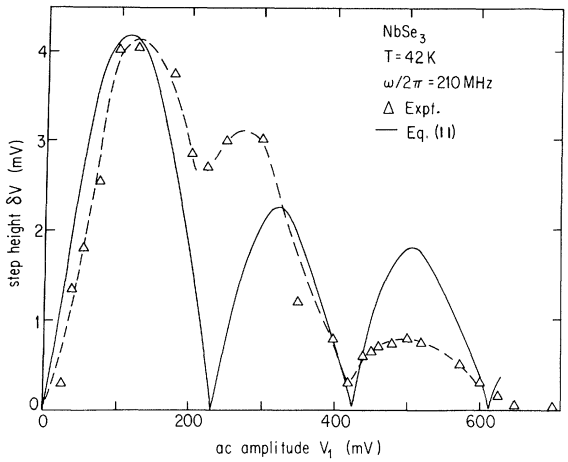

FIG. 12. Step height δV vs amplitude V_{ac} of the applied rf signal. rf frequency is 210 MHz and the step index $n=1$ (see text). Solid line is Eq. (11) with parameters given in the text. Dashed line is a guide for the eye for the experimental data.

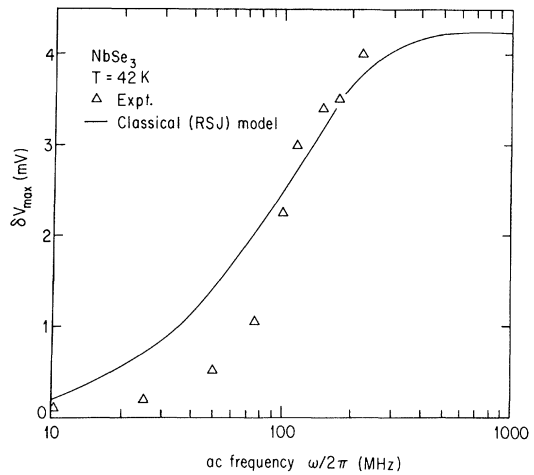

FIG. 13. Maximum step height δV_{max} attained vs rf frequency. Solid line is the prediction of the RSJ model of Josephson tunnel junctions (Ref. 37). Data of Figs. 2, 12, and 13 are for the same $NbSe_3$ sample.

chosen parameters $\omega_0^2\tau=503$ MHz and $\alpha=0.17$. V_T is fixed by experimental conditions at 24 mV. The positions of the maxima and minima of the Bessel function of Eq. (14) are in remarkably good agreement with the experimental data. The value of the crossover frequency $\omega_0^2\tau/2\pi$ deduced from this fit is 80 MHz, in good agreement with the value of 100 MHz obtained from the frequency dependence of the low-field ac conductivity alone (see Fig. 5). Equation (14), however, underestimates δV near the second peak in Fig. 11 and overestimates δV near the third peak. These peak heights are, however, quite sensitive to the pinning potential in Eq. (4), and a different choice of potential would distort somewhat the amplitudes of the peaks in the solution of δV. The value of $\alpha=0.17$ indicates that a large fraction of the sample is responding coherently to the external perturbation. Analysis of similar data for another sample yielded an even higher value of $\alpha=0.60$. Assuming that δV at the peak, as given by Eq. (14), is off at most by a factor of 2 (possibly arising from the relative closeness of the ac frequency $\omega/2\pi=210$ MHz to the crossover frequencies $\omega_0^2\tau/2\pi=100$ MHz), a value of $\alpha=0.60$ indicates that between 30% and 100% of the sample volume is phase coherent. The high coherence is in agreement with other studies of the current oscillations[15] and switching[38] phenomena of $NbSe_3$.

From data similar to that shown in Figs. 2 and 12, we find that the maximum height of the $n=1$ step, δV_{max}, is strongly frequency dependent. This is shown in Fig. 13 where δV_{max} is plotted as a function of ω. Since most of this data falls into the low-frequency solution regime of Eq. (4), we have in Fig. 13 plotted δV_{max} as calculated[37] for the RSJ model in the overdamped low-frequency limit. The value of $\omega_0^2\tau/2\pi=50$ MHz obtained from this fit is in good agreement with the result $\omega_0^2\tau/2\pi=80$ MHz deduced from the analysis of Fig. 12.

Equation (11) indicates that the $n=0$ step height, i.e., the threshold voltage V_T, should also display a Bessel-function oscillatory behavior. Such oscillations are not apparent from the data in Figs. 1 or 2 or from the more sensitive differential resistance data of Fig. 4 which shows that V_T goes smoothly to zero with increasing V_{ac}. This failure of Eq. (4) to predict the correct form of the I-V characteristics near threshold has been noted previously in studies[39] of the differential conductivity dV/dI, even in the absence of an applied ac field. We, however, remark that Eq. (4) appears to describe well the behavior of a CDW system below and above V_T, and fails only in the immediate vicinity of V_T. We shall return to the divergence problem of the classical model at threshold shortly.

On the basis of the analysis in Figs. 12 and 13 we conclude that the simple nonlinear Eq. (4) describes both the ac frequency and amplitude dependence of the dc response. The analysis also shows a highly coherent response where the whole specimen responds to ac and dc driving fields as nearly one coherent unit. This observation is highly suggestive of long-range phase coherence in the current-carrying CDW condensate.

Our analysis also leads to a strongly damped CDW response in the nonlinear, sliding CDW region. This observation is in accordance with the behavior of the frequency-dependent conductivity $\sigma_{ac}(\omega)$ when analyzed in terms of the classical equation. Although these experiments indicate an overdamped response always, we note that recent analysis of the coherent current oscillations[15] indicates that inertial effects may be important at driving fields well above the threshold field. Whether this apparent discrepancy is related to the differences in the measurement methods (pulse measurements were used to observe the current oscillations, while the present experiments are steady-state measurements), or reflect the deviation from a sinusoidal potential, or are due to an inherent deficiency of the classical model, remains to be seen.

B. Effect of dc fields on the ac response

As is evident from Figs. 5—8 the ac response of the CDW condensate is strongly modified by the application of applied dc bias fields. Broadly speaking, two effects

are important: First, the *overall* modification of the ac response (such as the overall decrease of the dielectric constant with increasing applied dc fields such as shown in Fig. 7), and second, the sharp interference effects observed at well-defined frequencies and (related) applied dc fields. The latter effects are clearly related to the coherent current-oscillation phenomena, and to the "Shapiro" steps described in the preceding section.

Both of these features are expected to be recovered by a calculation which is based on Eq. (4) and in which the ac response is evaluated. Owing to the inherent nonlinearity of the problem, analytic solutions are expected to be obtained only in certain limits, but not for the general case with a broad parameter range. We are also not aware of computer simulations of the phenomena displayed in Figs. 6–8. We proceed therefore with a semiqualitative analysis of our experimental findings. We first describe the overall dependence of $\mathrm{Re}\sigma_{\mathrm{ac}}(\omega)$ and $\mathrm{Im}\sigma_{\mathrm{ac}}(\omega)$ on the applied dc field and then proceed to discuss the interference phenomena.

In the absence of dc driving fields, Eq. (4) predicts an ac response to a small amplitude ($V_{\mathrm{ac}} \ll V_T$) ac driving field given by

$$\mathrm{Re}\sigma_{\mathrm{ac}}(\omega)=\frac{ne^2\tau}{m}\frac{1}{1+(\omega_0^2\tau/\omega)^2}\ , \tag{15}$$

$$\mathrm{Im}\sigma_{\mathrm{ac}}(\omega)=\frac{ne^2\tau}{m}\frac{\omega_0^2\tau}{\omega}\frac{1}{1+(\omega_0^2\tau/\omega)^2}\ , \tag{16}$$

and a low-frequency ac dielectric constant,

$$\epsilon(\omega\rightarrow 0)=\frac{4\pi ne^2}{m\omega_0^2}\ . \tag{17}$$

Equations (15)–(17) are for an overdamped system where inertial terms can be neglected. This limit is here appropriate since inertial terms lead to a decrease of $\mathrm{Re}\sigma_{\mathrm{ac}}(\omega)$ at moderate frequencies and to a negative dielectric constant, neither of which are observed in $NbSe_3$ up to microwave frequencies.

The solid and dotted lines in Fig. 5 are Eqs. (15) and (16) with parameters $\omega_0^2\tau/2\pi=100$ MHz and $ne^2\tau/m=0.85\sigma_{\mathrm{dc}}$. Combining these parameters with Eq. (17) and the measured low-frequency dielectric constant $\epsilon=2\times10^8$ leads to a classical pinning frequency $\omega_0=2\times10^{11}\ \mathrm{sec}^{-1}$.

In the presence of a dc bias V_{dc}, the ω-dependent ac response is expected to be modified in both the pinned ($V_{\mathrm{dc}}<V_T$) and in the depinned ($V_{\mathrm{dc}}>V_T$) CDW states. In the pinned CDW state an important parameter in the classical model is the restoring force constant k for the CDW. This parameter characterizes the ac dielectric constant $\epsilon(\omega)$. For a sinusoidal pinning potential as in Eq. (4) the depinning process at V_T is the consequence of the restoring force going to zero. This is reflected in the dielectric constant, and from Eq. (4) we find

$$\epsilon(\omega,V_{\mathrm{dc}})=\frac{\epsilon(\omega,V_{\mathrm{dc}}=0)}{[1-(V_T/V_{\mathrm{dc}})^2]^{1/2}}\ . \tag{18}$$

Thus the dielectric constant ϵ measured in the presence of a dc bias V_{dc} should diverge at the threshold V_T. As is evident from Fig. 7, a divergent dielectric constant is not observed in our experiments on $NbSe_3$, but rather ϵ is nearly independent of V_{dc} below V_T. In the sliding CDW region ϵ decreases with increasing electric field and tends to zero for $V\rightarrow\infty$. We remark that $\epsilon(V_{\mathrm{dc}},\omega)$, as calculated for the classical model assuming a *harmonic* potential, is independent of the bias V_{dc}.

To account for the decrease in ϵ with increasing V_{dc} above V_T, it is suggested that, for a moving CDW, there is a critical velocity v_c for the CDW above which an ac polarization at frequency $\omega/2\pi$ cannot be built up. Letting v_d denote the time-averaged drift velocity of the sliding CDW, the dielectric constant will be given by

$$\epsilon(\omega,V_{\mathrm{dc}})=\epsilon(\omega,V_{\mathrm{dc}}=0)[1-(v_d/v_c)]\ . \tag{19}$$

A reasonable estimate for the critical velocity is $v_c=\lambda\omega/2\pi$, where λ is the wavelength of the periodic pinning potential and ω is the frequency of the ac driving field. Again assuming a harmonic potential, the drift velocity is given by

$$V_d=\frac{2e\tau V_T}{m\ln[(V_{\mathrm{dc}}+V_T)/(V_{\mathrm{dc}}-V_T)]}\ . \tag{20}$$

By incorporating this result into the expression for $\epsilon(\omega,V_{\mathrm{dc}})$, Eq. (19), we find

$$\epsilon(\omega,V_{\mathrm{dc}})=\epsilon(\omega,V_{\mathrm{dc}}=0)\left[-1\frac{e\tau V_T 4\pi}{m\ln(V_{\mathrm{dc}}+V_T)/(V_{\mathrm{dc}}-V_T)}\right]\ . \tag{21}$$

Thus, neglecting interference effects, ϵ decreases with increasing applied bias V_{dc} above V_T and approaches zero for an applied V_{dc} which corresponds roughly to a noise frequency

$$f_1=\frac{2\pi\omega_0^2\tau}{\ln[(V_{\mathrm{dc}}+V_T)/(V_{\mathrm{dc}}-V_T)]}\ ,$$

as observed. Figure 14 shows Eq. (21) plotted for two values of ω along with the experimental results of

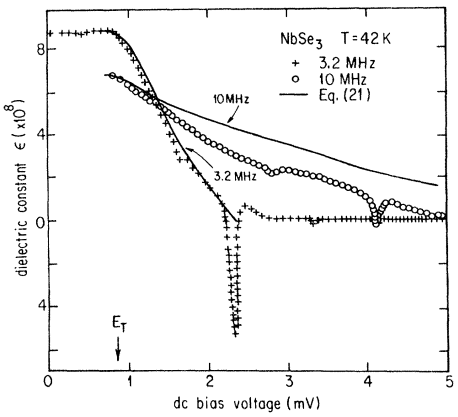

FIG. 14. Field-dependent ac dielectric constant $\epsilon(\omega)$ of $NbSe_3$ for two different values of the applied ac frequency $\omega/2\pi$. Solid lines are the predictions of Eq. (21).

$\epsilon(\omega, V_{dc})$ for $NbSe_3$ at $T=42$ K. Reasonable agreement is found between the predictions of Eq. (21) and experiment.

We note that the low-frequency dielectric constant has recently been calculated by Tucker[40] using Bardeen's tunneling theory. Tucker's calculation also reproduces the main features of our experimental findings. The calculation does not lead to a divergence in ϵ as $V \to V_T$, in agreement with the experiments. However, in its present form the calculation does not include the contribution of the pinned CDW mode.[27] Whether this mode would also lead to a divergent response at V_T remains to be seen.

Turning to the observation of sharp steps in $\mathrm{Re}\sigma_{ac}(\omega)$ and strong inductive dips $\epsilon(\omega)$, we shall employ arguments adapted from standard rf circuit theory. We shall attribute the steps in $\mathrm{Re}\sigma_{ac}(\omega)$ and the inductive dips in $\epsilon(\omega)$ observed in $NbSe_3$ as due to a classical phase locking between the applied ac excitation at frequency $\omega/2\pi$ and the coherent current oscillations at frequency f_1 (and $2f_1$, etc.). Direct observations of the coherent current oscillations in $NbSe_3$ have shown[15] that the phase of the current oscillations can always be synchronized to the start of a rectangular voltage pulse. The phase of the oscillating response is found to be $\pi/2$ with respect to the start of the pulse, *regardless* of the amplitude, width, or repetition rate of the pulse. It is therefore suggested that whenever the ac driving signal (which acts as a perturbation on the system) is at a frequency which equals a harmonic or subharmonic of f_1, the fundamental noise frequency and the phase of the coherent current oscillation locks on to the ac driving field with a phase difference of $\pi/2$.

The sample response to a purely ac low-amplitude driving field $V_{ac}\sin(\omega t)$ can be approximated by $R\sin(\omega t+\delta)$, where R is a constant and δ reflects the out-of-phase component of the response. A purely dc driving field with $V_{dc} > V_T$ will produce a current response $C+Ng(2\pi f_1 t+\phi)$ where C is the time-averaged response and g is a periodic function of time with period $(2\pi f_1)^{-1}$ and of unit amplitude. N represents the oscillation amplitude. Assuming independent behavior, the current response to a combined ac + dc driving field

$$V = V_{dc} + V_{ac}\sin(\omega t) \tag{22}$$

will be

$$I = R\sin(\omega t+\delta) + Ng(2\pi f_1 t+\phi)\ , \tag{23}$$

where the time-averaged component has been subtracted. Approximating the coherent current oscillation by a sinusoidal function, and assuming $\omega/2\pi = f_1$ for strongest interference, we obtain a response

$$I = R\sin(\omega t+\delta) + N\sin(\omega t+\phi)\ . \tag{24}$$

As discussed earlier, the strong inductive dip in ϵ corresponds to a bias voltage V_{dc} where, in the absence of interference effects, ϵ is approximately zero. Thus to analyze this dip we may set $\delta=0$ in Eq. (24). The total phase difference between the ac driving field and the response is then given by

$$\beta = \tan^{-1}\left[\frac{N\sin\phi}{R+N\cos\phi}\right]\ . \tag{25}$$

Setting the phase-locking angle ϕ equal to the empirically determined value $\pi/2$, and using for R and N the measured response amplitudes $R=0.7$ mV and $N=0.1$ mV, we obtain $\beta=-0.14$, which corresponds to a 4-MHz value of the dielectric constant $\epsilon=-7.66\times10^8$, in good agreement with the measured 4-MHz value of $\epsilon=-5.5\times10^8$ at the center of the inductive dip in Fig. 7. A similar analysis for the real part of the conductivity $\mathrm{Re}\sigma_{ac}(\omega)$ predicts a step height $\Delta\sigma/\sigma_0=1.5$ for the 4-MHz step at $v_{dc}=2.3$ mV which again agrees favorably with the measured step height $\Delta\sigma/\sigma_0=1.3$ obtained from Fig. 6.

The finite widths of the steps in $\mathrm{Re}\sigma_{ac}(\omega)$ and of the inductive dips in $\epsilon(\omega)$, as seen in Figs. 6 and 7, indicate that the interference effects are obtained over a small but finite range of noise frequencies for fixed $\omega/2\pi$. In a discussion of related synchronization effects in the differential resistivity of $NbSe_3$, Richard *et al.*[41] have calculated the frequency width for which frequency locking will occur in a single domain. They obtain the model-independent expression for the extreme V_{dc} value

$$V_{dc} - V_A = V_T(V_{ac}/2V_A)\ , \tag{26}$$

where V_A is that dc bias field which yields a fundamental noise frequency equal to $\omega/2\pi$, the external ac frequency. Equation (26) predicts a width of the strong inductive dip in $\epsilon(\omega/2\pi=4$ MHz, $V_{dc}=2.3$ mV) of $2(V_{dc}-V_A) = V_T(V_1/V_A)=0.27$ mV, in excellent agreement with the observed width of 0.26 mV from Fig. 7.

The strong interference effects observed in $NbSe_3$ are thus adequately explained in terms of classical electromagnetic interference phenomena. Whether such interference effects are intrinsic to the tunneling model remains to be seen.

C. Relation between the CDW current and fundamental frequency f_1

From the discussion in the previous sections it is clear that in $NbSe_3$ the coherent current oscillations play a fundamental role in the dc and ac response characteristics of the sample. We shall further investigate here the relation between the fundamental noise frequency f_1 and the excess CDW current I_{CDW}.

In the nonlinear conductivity region of $NbSe_3$ the current response due to an applied dc voltage contains an ac component. We define the dominant oscillation frequency of this component as f_1, the fundamental noise frequency. From Fig. 9 we see that a plot of f_1 vs I_{CDW} yields an absolutely linear relationship, i.e., $I_{CDW}=kf_1$, where k is a constant of proportionality. In a very general sense we may write the time-averaged excess current as

$$I_{CDW} = n(T)ev_dA\ , \tag{27}$$

where $n(T)$ is the density of electrons condensed in the CDW mode, v_d is the CDW drift velocity, and A is the cross-sectional area of the sample. Setting $v_d=f_1\lambda$, where λ is a characteristic distance, we easily obtain a linear relation between I_{CDW} and f_1,

$$I_{CDW} = e\lambda An(T)f_1\ . \tag{28}$$

This relation was first proposed by Monceau *et al.*[16] on experimental grounds, and it is also predicted by the classical model of CDW transport, Eq. (4). Equation (28) allows us to determine directly $n(T)$, and hence also the order parameter $\Delta(T)$ from the experimentally determined slope $I_{\rm CDW}/f_1$ as shown in Fig. 11. Also shown in Fig. 11 is the order parameter as determined from the BCS gap expression and from the x-ray amplitude as determined by Fleming *et al.*[42] Although the scatter in $I_{\rm CDW}/f_1$ is somewhat large at lower temperatures, this ratio is in general agreement with $n(T)$ as determined from structural data and theoretical considerations.

It should be noted that the linear relation between $I_{\rm CDW}$ and f_1 is not always observed in $NbSe_3$. For some $NbSe_3$ samples a slope $I_{\rm CDW}/f_1$ is found which increases with increasing bias field. This field has also been observed by Richard *et al.*[41] in $NbSe_3$ and also by ourselves in TaS_3.[43] The effect appears to reflect the extent to which the sample volume is phase coherent; for samples with visible structural defects such as stranding near the contacts or nonuniform cross-sectional areas, the nonlinearity of $I_{\rm CDW}/f_1$ is especially dramatic. The highly linear relation between $I_{\rm CDW}$ and f_1 observed in Fig. 9 is again strong evidence that in this high-quality $NbSe_3$ specimen the sample volume is acting as a single coherent unit with a single degree of freedom.

From Eq. (28) we see that if A and $n(T)$ are known along with $I_{\rm CDW}/f_1$, the characteristic length λ can be explicitly determined. Since the density of electrons condensed in the CDW state is given by $n(T=0)=2k_F/\pi$, we may rewrite Eq. (28) as

$$\frac{I_{\rm CDW}}{f_1}=2e\frac{n(T)}{n(T=0)} \tag{29}$$

per chain. Equation (29) applies to charge transport by CDW's. It has, however, recently been suggested by Bak[44] that the narrow-band noise observed in $NbSe_3$ is not due to sliding CDW's, but rather due to motion of a soliton lattice. In Bak's model[44] the peaks in the oscillating component of $I_{\rm CDW}$ represent motion of individual solitons past the current detector at the end of the sample. For $NbSe_3$ the assumed solitons are predicted to carry a fractional charge $e^*=e/2$, and thus Eq. (29) must be modified to read

$$\frac{I_{\rm sol}}{f_1}=\frac{e}{2}\frac{n(T)}{n(T=0)} \tag{30}$$

per chain.

Another theory of CDW transport by Barnes and Zawadowski[45] which treats the left- and right-going components of the incommensurate CDW as two macroscopic quantum states, suggests that quantum oscillations may be responsible for the narrow-band noise. For various choices of sample parameters, this theory predicts an effective charge unit $e^*=e$, which leads to

$$\frac{I_{\rm CDW}}{f_1}=e\frac{n(T)}{n(T=0)} \tag{31}$$

per chain.

One should clearly be able to determine which of Eqs. (29)—(31) is most appropriate to $NbSe_3$ by careful measurements of $I_{\rm CDW}/f_1$. However, this must be done on a per-chain basis, and also $n(T)$ must be well established. Although the ratio $I_{\rm CDW}/f_1$ has been measured quite accurately in $NbSe_3$ at selected temperatures (see, for example, Fig. 9), the exact number of chains participating in the conduction process is not well defined for a particular sample due to ambiguities in the sample dimensions. This is in part due to the rather fibrous morphology of the material, which makes an accurate measurement of the cross-sectional area of a sample difficult. In addition a reliable absolute value of $n(T=0)$ has not been determined, due to the two-dimensional character of $NbSe_3$, which prevents complete Fermi-surface destruction at T_P. Owing to these uncertainties, we are at present not able to unequivocably establish which of Eqs. (29)—(31) is most appropriate to $NbSe_3$. However, experiments[43] on orthorhombic TaS_3, where $n(T=0)$ and the absolute dc resistivity are less ambiguous, have indicated that $I_{\rm CDW}/f_1=2e\ n(T)/n(T=0)$, as predicted by Eq. (29). In this case then λ corresponds to the wavelength of the CDW, and rules out soliton-dominated transport.

IV. CONCLUSIONS

Experiments reported in this paper indicate that in the CDW state of $NbSe_3$ in the nonlinear conductivity region the specimen responds to joint ac and dc driving fields in a highly coherent manner. The analysis of the ac-induced steps in the dc I-V characteristics leads to an effective volume which is between 30% and 100% of the volume of the specimen, and a similar highly coherent response is obtained from the analysis of the ac conductivity in the presence of dc applied fields. These observations, together with the direct observations of the current oscillations which show that just above threshold the total CDW current is oscillating,[14,15] strongly suggest that long-range phase coherence exists in the current-carrying CDW state.

A simple nonlinear equation representing the CDW as a classical particle moving in a periodic potential[18] describes well the various types of ac-dc interference effects, and also the overall behavior of the frequency-dependent conductivity both in the presence and in the absence of applied dc fields. An electrical analog, the relaxation oscillator,[22] has rather similar features and is also expected to describe our experimental findings. Both models, however, lead also to spurious divergences, which are not observed by experiment. The simple nonlinear equation, Eq. (4), leads to a divergence in the differential conductance, and the differential dielectric constant also diverges at the threshold field E_T for the onset of nonlinear conduction. Although different forms of the periodic potential lead to different power laws near E_T, the divergent dI/dV and $d\epsilon/dV$ is a universal feature of all such models.

A distribution of pinning potentials within the sample would lead to the removal of the divergences near E_T. Such models that would, however, do not lead to a highly coherent response at applied voltage close to V_T, in contrast to the experimental observations. Recent computer simulations[46] of the CDW depinning process which include internal degrees of freedom of the CDW have led to the removal of the divergence with narrow-band noise

peaks still observed. Whether such calculations lead to a quantitative account of the experimental findings remains to be seen.

We also note that a tunneling model proposed by Bardeen[23] leads to frequency- and field-dependent transport phenomena with the overall behavior of $\sigma_{ac}(E)$ and $\sigma_{ac}(\omega)$ similar to that observed experimentally. Although the model in its original form does not account for the current oscillations, the assumption of highly coherent motion of the CDW over the hills and valleys of the pinning potential leads[15] also to current oscillations, with the relation between I_{CDW} and f_1 as given by Eq. (2). We expect that any model which accounts for $\sigma_{dc}(E_{dc})$ [and $\sigma_{ac}(\omega)$] and for the current oscillations will also account for experiments performed in the presence of joint ac and dc excitations. We believe therefore that a description of our experiments is also possible within the framework of the tunneling model.[23]

With a highly coherent response including the total volume of the specimen, the effects of the sample size and the boundaries associated with the contacts have to be examined in detail. It is expected that such effects play an especially important role in samples with a small volume or short length. We have therefore measured the threshold voltage V_T for a sample where the distance between the contact leads was reduced after each successive experiment. For v_T determined by an intrinsic length scale one expects that the threshold field $E_T = V_T/l$ is no longer independent of l, where l is the length of the sample. Only when the intrinsic length scale is much smaller than the sample length is E_T independent of l. In a phenomenological way we may write

$$V_T = E_T l + V_0 = E_T(l + l_0) , \tag{32}$$

where l_0 is the intrinsic length scale. Figure 15 shows V_T vs l measured at temperature $T = 32$ K. The overall behavior of $V_T(l)$ is roughly described by Eq. (32), and a least-squares fit of our experimental data leads to $l_0 = 0.2$ mm. Similar experiments performed in TaS_3 (Ref. 47) lead to values of l_0 of similar magnitude. The experiments reported in this paper have been performed in materials where $l > l_0$, and we believe therefore that finite-size effects do not play an important role here.

We conclude that long-range coherence is an important factor in CDW transport and accounts for a broad variety of experimental observation in the presence of joint ac and dc driving fields. Other observations, such as a finite-threshold field observed in long samples with concentration dependence either linear or quadratic[48] and broad-band noise in the current-carrying state,[1] point to the importance of the local deformations. Both long-range coherence and local deformations appear to play an important role in the statics and dynamics of CDW's. The most likely explanation for this behavior is that the characteristic length scales which determine the decay of the phase correlations is not much smaller than the size of the specimens. If this is the case, the samples can be regarded as containing a finite number of domains. Detailed studies of the phenomena reported here as a function of volume of the specimens may clarify this point.

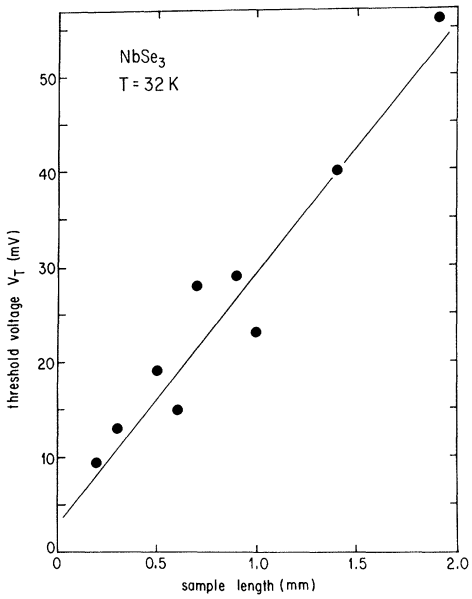

FIG. 15. Threshold voltage V_T vs distance l between the voltage leads for $NbSe_3$ at $T = 32$ K. Full line is Eq. (33) with $l_0 = 0.2$ mm.

ACKNOWLEDGMENTS

We wish to thank R. M. Fleming for providing the $NbSe_3$ samples and John Bardeen, T. Holstein, R. A. Klemm, J. R. Schrieffer, and A. Zawadowski for useful discussions. This research was supported by the National Science Foundation under Grant No. DMR-81-3085. One of us (A.Z.) received support from the Exxon Education Foundation.

[1]For a review, see R. M. Fleming, in *Physics in One Dimension*, Vol. 23 of *Springer Series in Solid State Sciences*, edited by J. Bernasconi and T. Schneider (Springer, Berlin, 1981); N. P. Ong, Can. J. Phys. 60, 757 (1982); G. Grüner, Comments Solid State Phys. 10, 183 (1983).

[2]A. H. Thompson, A. Zettl, and G. Grüner, Phys. Rev. Lett. 47, 64 (1981); M. Ido, K. Kawabata, T. Sambongi, K. Yamaya, and Y. Abe, Mol. Cryst. Liq. Cryst. 81, 91 (1982).

[3]A. Zettl, C. M. Jackson, A. Janossy, G. Grüner, A. Jacobsen, and A. H. Thompson, Solid State Commun. 43, 345 (1982).

[4]See, for example, *Highly Conducting One Dimensional Solids*, edited by J. T. Devreese, R. P. Evrard, and V. E. Van Doren (Plenum, New York, 1979).

[5]P. A. Lee, T. M. Rice, and P. W. Anderson, Solid State Commun. 14, 203 (1974).

[6]For a short review, see J. A. Berlinsky, Rep. Prog. Phys. 42, 1243 (1980).

[7]J. W. Brill, N. P. Ong, J. C. Eckert, J. W. Savage, S. K. Khanna, and R. B. Sonoamo, Phys. Rev. B 23, 1517 (1981); W. W. Fuller, G. Grüner, P. M. Chaikin, and N. P. Ong, Phys. Rev.

B 23, 6259 (1981).
[8]Pei-Ling Hsieh, F. de Czito, A. Janossy and G. Grüner, J. Phys. (Paris) (in press).
[9]P. A. Lee and T. M. Rice, Phys. Rev. B 19, 3970 (1979).
[10]G. Grüner, L. C. Tippie, J. Sanny, W. G. Clark, and N. P. Ong, Phys. Rev. Lett. 45, 935 (1980); S. W. Longcor and A. M. Portis, Bull. Am. Phys. Soc. 25, 340 (1980).
[11]A. Zettl and G. Grüner, Phys. Rev. B 25, 2081 (1982).
[12]H. Frölich, Proc. R. Soc. London Ser. A 223, 296 (1954).
[13]R. M. Fleming and C. C. Grimes, Phys. Rev. Lett. 42, 1423 (1979).
[14]R. M. Fleming, Solid State Commun. 43, 167 (1982).
[15]John Bardeen, E. Ben-Jacob, A. Zettl, and G. Grüner, Phys. Rev. Lett. 49, 493 (1982).
[16]P. Monceau, J. Richard, and M. Renard, Phys. Rev. Lett. 45, 43 (1980).
[17]G. Grüner, Mol. Cryst. Liq. Cryst. 82, 17 (1982).
[18]G. Grüner, A. Zawadowski, and P. M. Chaikin, Phys. Rev. Lett. 46, 511 (1981).
[19]P. Monceau, J. Richard, and M. Renard, Phys. Rev. B 25, 931 (1982).
[20]P. A. Lee and T. M. Rice, Phys. Rev. B 19, 3970 (1979).
[21]G. Grüner, W. G. Clark, and A. M. Portis, Phys. Rev. B 24, 7247 (1981).
[22]M. Weger, G. Grüner, and W. G. Clark, Solid State Commun. (in press); J. Phys. (Paris) (in press).
[23]John Bardeen, Phys. Rev. Lett. 42, 1498 (1979); 45, 1978 (1980); Mol. Cryst. Liq. Cryst. 81, 1 (1981).
[24]J. R. Tucker, IEEE J. Quantum Electron. QE-15, 1234 (1979).
[25]J. R. Tucker, J. H. Miller, K. Seeger, and John Bardeen, Phys. Rev. B 25, 2979 (1982).
[26]K. Seeger, W. Mayr, and A. Philipp, Solid State Commun. 43, 113 (1982).
[27]G. Grüner, A. Zettl, W. G. Clark, and John Bardeen, Phys. Rev. B 24, 7247 (1981).
[28]D. E. McCumber, J. Appl. Phys. 39, 3113 (1968); W. C. Stewart, Appl. Phys. Lett. 12, 277 (1968).
[29]E. Ben-Jacob (unpublished); S. N. Artemenko and A. F. Volkov, Zh. Eksp. Teor. Fiz. 80, 2018 (1980) [Sov. Phys.—JETP 53, 1050 (1981)].
[30]See, for example, P. Lindelof, Rep. Prog. Phys. 44, 949 (1981).
[31]A. Zettl and G. Grüner, Solid State Commun. 46, 501 (1983).
[32]G. Grüner and A. Zettl, J. Phys. (Paris) (in press).
[33]A. Zettl and G. Grüner (unpublished).
[34]S. Shapiro, Phys. Rev. Lett. 11, 80 (1963).
[35]P. L. Richards, in *Semiconductors and Semimetals,* edited by R. K. Willardson and A. C. Beer (Academic, New York, 1977), Vol. 12.
[36]R. L. Kautz, J. Appl. Phys. 52, 3528 (1981); V. N. Belykh, N. F. Pedersen, and O. H. Soerensen, Phys. Rev. B 16, 4853 (1977); 16, 4860 (1977); E. Ben-Jacob, Y. Braiman, R. Shainsky, and Y. Imry, Appl. Phys. Lett. 38, 822 (1981).
[37]H. Fack and V. Kose, J. Appl. Phys. 42, 320 (1971); T. D. Clark and P. E. Lindelof, Phys. Rev. Lett. 37, 368 (1976).
[38]A. Zettl and G. Grüner, Phys. Rev. B 26, 2298 (1982).
[39]A. Zettl, G. Grüner, and A. H. Thompson, Phys. Rev. B 26, 5760 (1982).
[40]J. R. Tucker (private communication).
[41]J. Richard, P. Monceau, and M. Renard, Phys. Rev. B 25, 948 (1982).
[42]R. M. Fleming, D. E. Moncton, and D. B. McWhan, Phys. Rev. B 18, 5560 (1978).
[43]A. Zettl and G. Grüner, Phys. Rev. B 28, 2091 (1983).
[44]Per Bak, Phys. Rev. Lett. 48, 692 (1982).
[45]S. E. Barnes and A. Zawadowski, Phys. Rev. Lett. 51, 1003 (1983).
[46]L. Pietronero and S. Strässler (unpublished).
[47]G. Mihaly (unpublished).
[48]J. W. Brill, N. P. Ong, J. C. Eckert, J. W. Savage, S. K. Khanna, and R. B. Somoano, Phys. Rev. B 23, 1517 (1981).